



## Weak localization and size effects in thin $\text{In}_2\text{O}_3$ films prepared by autowave oxidation



Igor A. Tambasov <sup>a,\*</sup>, Anton S. Tarasov <sup>a,b</sup>, Mikhail N. Volochaev <sup>a,c</sup>, Mikhail V. Rautskii <sup>a</sup>, Victor G. Myagkov <sup>a</sup>, Liudmila E. Bykova <sup>a</sup>, Victor S. Zhigalov <sup>a,c</sup>, Alexey A. Matsynin <sup>a</sup>, Ekaterina V. Tambasova <sup>c</sup>

<sup>a</sup> Kirensky Institute of Physics, Siberian Branch of the Russian Academy of Sciences, Akademgorodok 50, 660036 Krasnoyarsk, Russia

<sup>b</sup> Siberian Federal University, Svobodny Prospect 79, 660041 Krasnoyarsk, Russia

<sup>c</sup> Reshetnev Siberian State Aerospace University, Krasnoyarsk Worker 31, 660014 Krasnoyarsk, Russia

### HIGHLIGHTS

- The magnetoresistance of the thin  $\text{In}_2\text{O}_3$  film was  $-1.35\%$  at a temperature 4.2 K.
- Negative magnetoresistance has been explained by the weak localization theory.
- The temperature dependence of phase-coherence length  $l_\phi$  began to oscillate at 30 K.
- The oscillation of  $l_\phi$  can be used to evaluate the structural features of thin films.

### ARTICLE INFO

#### Article history:

Received 24 February 2016

Received in revised form

30 May 2016

Accepted 7 June 2016

Available online 7 June 2016

#### Keywords:

Thin indium oxide films

Weak localization

Electron-electron interaction

Disordered semiconductors

Nanostructured films

Phase-coherent length

### ABSTRACT

The negative magnetoresistance of thin  $\text{In}_2\text{O}_3$  films, obtained by an autowave oxidation reaction, was detected within a temperature range of 4.2–80 K. The magnetoresistance was  $-1.35\%$  at a temperature of 4.2 K and an external magnetic field of 1 T. A weak localization theory was used to explain the negative magnetoresistance and to determine the phase-coherence length in a temperature range of 4.2–80 K. The phase-coherence length was found to oscillate as the temperatures increased to around 30 K. From the maximum and minimum values of the oscillation of the phase-coherence length, it was suggested that the  $\text{In}_2\text{O}_3$  film has two structure characteristic parameters. Transmission electron microscopy showed the structure of the thin  $\text{In}_2\text{O}_3$  film to have structural features of a «crystal phase – amorphous phase». It was found that the crystalline phase characteristic size was consistent with the maximum phase-coherence length and the amorphous phase characteristic size was consistent with the minimum phase-coherence length. It has been suggested that the temperature measurements of the magnetoresistance and the theory of weak localization can be used to evaluate the structural features of nanocomposite or nanostructured thin films.

© 2016 Elsevier B.V. All rights reserved.

### 1. Introduction

Magneto-transport properties of thin transparent conductive oxide (TCO) films with different compositions are intensively studied at present time [1–4]. Furthermore, nanocomposite films based on transparent conductive oxides are also being investigated [5–7]. In many cases, these studies are carried out in a wide temperature range. The determination of magnetoresistance (MR) as a function of temperature and film composition is the main

basis of these studies, since magnetoresistance is a very useful characteristic when creating electronic device [8,9]. Moreover, for fundamental and applied problems, it is very important to know the optical, electrical and magnetic properties of  $\text{In}_2\text{O}_3$  and compounds on its basis in a wide temperature range. This is because indium oxide films are the most demanded among the TCO. In particular, at low temperatures, information about the electrical and magnetoresistive properties of indium oxide can give additional insight on quantum transport in low-dimensional systems [10]. At high temperatures, comparable to room temperature, nonlinear optical properties of indium tin oxide films can be used to create devices for nanophotonics, plasmonics, and nonlinear

\* Corresponding author.

E-mail address: [tambasov\\_igor@mail.ru](mailto:tambasov_igor@mail.ru) (I.A. Tambasov).

nano-optics [11]. As another example, nanocomposite thin Fe –  $\text{In}_2\text{O}_3$  films, which have high magnetization at temperature room, can be used as a material for creating spintronic devices [12].

The presence of the magnetoresistance at low temperatures and its absence at room temperature in materials may be associated with quantum transport [13]. The presence of negative magnetoresistance can be caused by a variety of quantum electronic effects [10]. Recently, the negative magnetoresistance has been observed at low temperatures for pure and doped TCO films. For example, it was shown that pure and Cu doped ZnO films have a negative magnetoresistance [14]. Al doped ZnO films grown by atomic layer deposition also had a negative magnetoresistance [15]. Other thin TCO films such as indium tin oxide [16–18], B-doped ZnO [19], phosphorus-doped ZnO [20] and tin oxide [21,22] demonstrated a similar dependence of magnetoresistance on a magnetic field.

Disorder in semiconductors can be created by film growth [23–25] or doping [26]. In disordered semiconductors, where there is a large amount of impurities or defects, electrons in diffuse mode can have multiple scatterings from impurities or defects without a loss of energy that is the elastic collision. Since electrons have their own wave functions, it is probable that interference processes of the wave functions can occur upon elastic collision. Thus, the quantum-interference phenomena can be observed.

The quantum-interference phenomena include weak localization (WL) [13,27], electron-electron interactions [28] and, if there is notable spin-orbital coupling, weak antilocalization [29]. Moreover, universal conductance fluctuations [30], Aharonov-Bohm oscillations [31] and Altshuler-Aronov-Spivak oscillations [32,33] can be implemented on structured materials with particular dimensions.

The weak localization originates from the constructive interference of the backscattered electronic wave functions along time-reversal-symmetric paths. The constructive interference increases the probability of localizing an electron, manifesting itself as a positive correction to the resistivity at a zero magnetic field, which is easily broken under a non-zero external magnetic field since the constructive interference is reduced [34]. For this reason, weak localization can be responsible for the negative magnetoresistance in TCO and other materials. Moreover, the dimension of a system is significant for weak localization from the point of view of the observed magnetoresistance magnitude.

A characteristic parameter of weak localization and the other quantum-interference effects mentioned above is the phase-coherence length  $l_\phi$ , which determines the length at which there is a complete destruction of the phase coherence of electrons. It should be noted that a confirmation that the system can manifest the weak localization effect is the presence of a metal-semiconductor transition (MST) or a limited ratio of resistances measured at several K and room temperatures, respectively [15].

Recently, we proposed autowave oxidation as a new method of manufacturing thin indium oxide films [35]. In addition, the indium oxide film had a limited ratio of resistances measured at 5 K and 272 K ( $\sim 1.2$ ). Furthermore, it has been shown that ultraviolet irradiation can induce MST in the indium oxide film [36]. Thus, we expect that the weak localization effect and the related negative magnetoresistance can be observed in thin  $\text{In}_2\text{O}_3$  films prepared by autowave oxidation.

Here we present measurements of magnetoresistance up to 1 T in the temperature range 4.2–80 K and measurements of the structural features of the thin  $\text{In}_2\text{O}_3$  films observed by transmission electron microscopy (TEM). And most importantly, we found the temperature dependence of phase-coherence length to oscillate. This oscillation can be used to evaluate the structural features of the nanocomposite indium oxide film.

## 2. Material and methods

Thin indium oxide films were prepared by the autowave oxidation reaction [35]. The initial  $\text{In} + \text{In}_2\text{O}_3$  films were obtained by thermal evaporation of pure indium (99.999%) at a pressure of 1.5 Torr. The films were deposited on cover glass at room temperature. Prior to deposition, the substrates were cleaned in an ultrasonic bath with acetone and then methanol. Autowave oxidation reactions were carried out by heating the initial  $\text{In} + \text{In}_2\text{O}_3$  films with a speed of  $> 1 \text{ K/s}$ , to a temperature of 200 °C at a pressure of 0.5 Torr. After reaching the initiation temperature,  $T_0 \approx 180$  °C, the nucleation of the  $\text{In}_2\text{O}_3$  phase began, spreading over the surface in a self-sustaining manner. It has been shown that after the autowave oxidation, thin  $\text{In}_2\text{O}_3$  films had a homogenous surface with a crystallite size of 20–40 nm. The ratio of In/O was also homogenous on the film thickness. X-ray diffraction has revealed that the thin film only had the bixbyite crustal structure of  $\text{In}_2\text{O}_3$  [35]. It should be noted that we have not been able to obtain epitaxial indium oxide films by autowave oxidation because it is very difficult to synthesize epitaxial  $\text{In}_2\text{O}_3$  by the physical evaporation method [37].

The magnetoresistances were investigated from 4.2 to 80 K using a standard four-probe method. Pt contacts on top of the thin  $\text{In}_2\text{O}_3$  film were used and sputtered using an Emitech k575x sputter coater. The thickness of the Pt contacts was approximately 80 nm. The temperature dependence measurements of the magnetoresistance were performed using an original facility based on a helium cryostat, an electromagnet, and a precise Keithley-2400 current/voltage source meter [38].

The thickness and structural features of the thin  $\text{In}_2\text{O}_3$  films were measured by high-resolution TEM. For this purpose, cross-sectional TEM specimens were prepared by a focused ion of 40 keV  $\text{Ga}^+$  beam system (FIB) Hitachi FB-2100. A Ge protective layer was selected and formed by thermal deposition at room temperature. The Ge layer is necessary to protect the  $\text{In}_2\text{O}_3$  sample from structural degradation during FIB preparation and to improve contrast from the  $\text{In}_2\text{O}_3$  film in the TEM images. TEM images were acquired with a Hitachi HT7700 microscope operating at 110 kV.

## 3. Results and discussion

**Fig. 1** shows the dependence of resistance measured at zero and 0.6 T magnetic fields in a temperature range of 6.5–100 K. From **Fig. 1**, it can be estimated that the resistances begin to diverge at  $\sim 80$  K. It is clear that there is a negative magnetoresistance in the thin  $\text{In}_2\text{O}_3$  film.

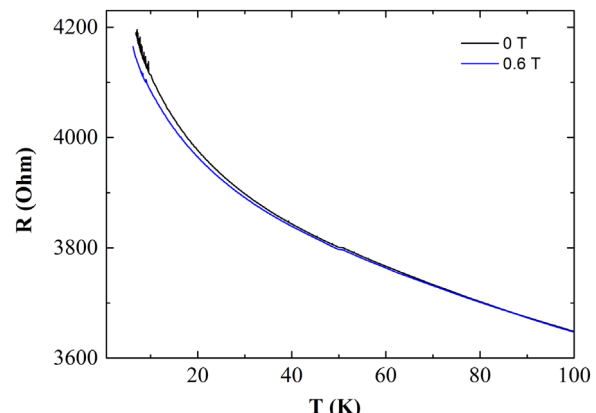


**Fig. 1.** The resistance temperature dependence of the thin  $\text{In}_2\text{O}_3$  film measured at external zero and 0.6 T magnetic fields in the film plane.

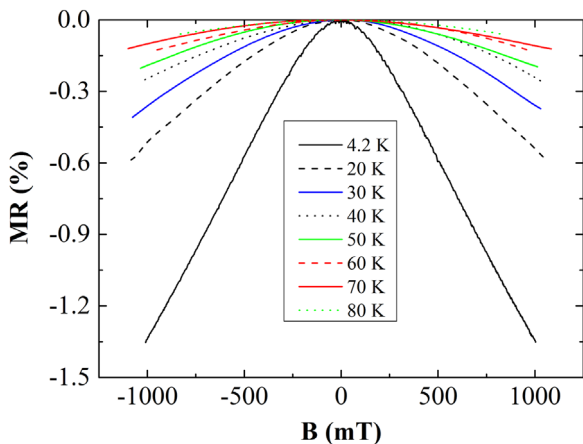


**Fig. 2.** The magnetoresistance of the thin In<sub>2</sub>O<sub>3</sub> film versus the external magnetic field measured in the temperature range 4.2–80 K.

Furthermore, there is slight change in the resistance of the films with a magnetic field. The slight change of the resistance in a magnetic field at low temperatures is characteristic of the weak localization effect [39–41].

The magnetoresistance dependencies on the magnetic field ( $B$ ) in the temperature range 4.2–80 K are shown in Fig. 2. It should be noted that the magnetoresistance has been defined as  $MR(\%) = \left[ \frac{R(B) - R(0)}{R(0)} \right] \times 100\%$ , where  $R(B)$  is resistance with a magnetic field and  $R(0)$  is resistance without a magnetic field. As seen from Fig. 2, the absolute value of the magnetoresistance is increasing as the temperature decreases. At a temperature of 4.2 K and an external magnetic field of 1 T the thin In<sub>2</sub>O<sub>3</sub> film magnetoresistance was –1.35%.

Negative MR in TCO is often observed in the weak localization regime. Furthermore, such cases are usually observed at low temperatures [15,24]. An understanding of the experimental data based on the WL model requires the existence of extended states at low temperatures. In 2-D, the sheet resistance is related to  $k_F l$  as

$$k_F l = \frac{\hbar/e^2}{R_{sheet}} \approx \frac{25 \text{ k}\Omega/\square}{R_{sheet}} \quad (1)$$

where  $k_F$  is the Fermi wave vector,  $l$  is the mean free path,  $\hbar$  is the Planck constant,  $e$  is the electron charge,  $R_{sheet}$  is the sheet resistance. The theory of WL is applicable for disordered materials with  $k_F l \gg 1$  [21]. For our case, the calculated value of  $k_F l$  was 5.95. As a result, the studied In<sub>2</sub>O<sub>3</sub> film is in the weak localization regime.

In 2-D, as shown in experimental studies [21,42], the magnetoresistance at the external parallel and perpendicular fields to the

film plane is the same. However, according to theoretical [43,44] and experimental studies [45,46], the magnetoresistance for parallel and perpendicular fields is anisotropic. Furthermore, anisotropic magnetoresistance can be observed for the 3D weak localization regime [34]. It was shown that a system dimension, from the point of view of the weak localization theory, can effectively be changed by the temperature [47,48]. In order to understand the influence of the magnetic field orientation on the magnetoresistance at different temperatures, we measured the magnetoresistance of the indium oxide film with the external perpendicular and parallel fields at 5 and 80 K. These magnetoresistance measurements are shown in Fig. 3.

Fig. 3 shows that the thin In<sub>2</sub>O<sub>3</sub> film magnetoresistance is isotropic at 5 and 80 K and we will discuss this result further down.

For analysis and comparison, we have used 2D and 3D weak localization theory to extract the phase-coherence length from the thin indium oxide thin magnetoresistance.

For the 2D WL regime, the expression for negative MR is given by [21,49]

$$MR(\%) = -\alpha \frac{e^2 R \square}{2\pi^2 \hbar} \left[ \psi\left(\frac{1}{2} + \frac{B_\phi}{B}\right) + \ln\left(\frac{B}{B_\phi}\right) \right] \times 100\% \quad (2)$$

where  $B_\phi = \hbar/4el_\phi^2$  is the inelastic scattering field and  $B$  is the applied magnetic field.  $R \square$  is the resistance per square,  $\alpha$  is a parameter in the renormalization group and  $\psi(x)$  is the digamma function.

The expression for the 3D WL negative MR is given by [40]

$$MR(\%) = -\alpha \frac{e^2 R \square}{2\pi^2 \hbar} \sqrt{\frac{eB}{\hbar}} f_3(\delta) \times 100\% \quad (3)$$

where  $\delta = B_\phi/B$ . The function  $f_3(\delta)$  used in Eq. (3) is given by [40]

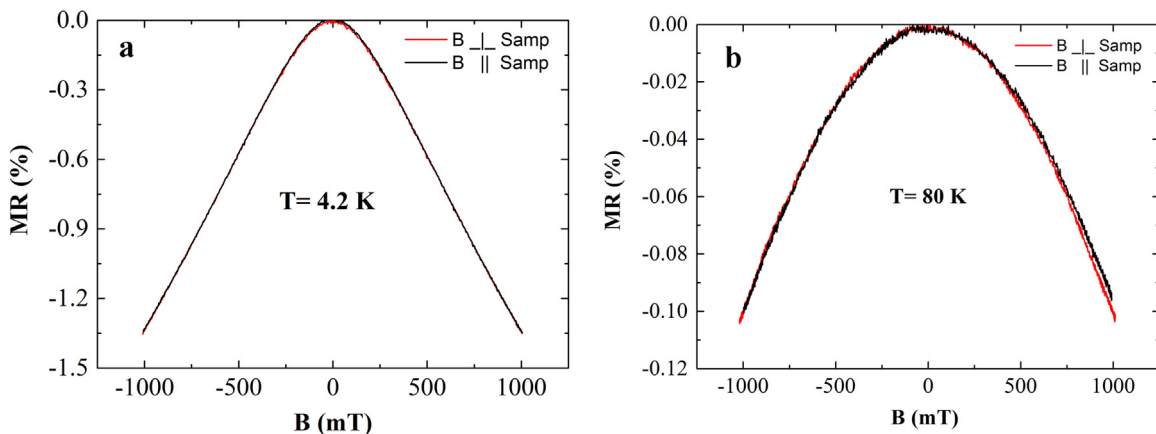
$$f_3(\delta) = \sum_{N=0}^{\infty} \left[ 2\left(\sqrt{N+1+\delta} - \sqrt{N+\delta}\right) - \frac{1}{\sqrt{N+1/2+\delta}} \right] \quad (4)$$

Experimental MR data was fitted to Eqs. (2) and (3) using  $\alpha$  and  $B_\phi$  as fitting parameters. Fig. 4 shows the experimental MR and the corresponding fit using Eq. (2).

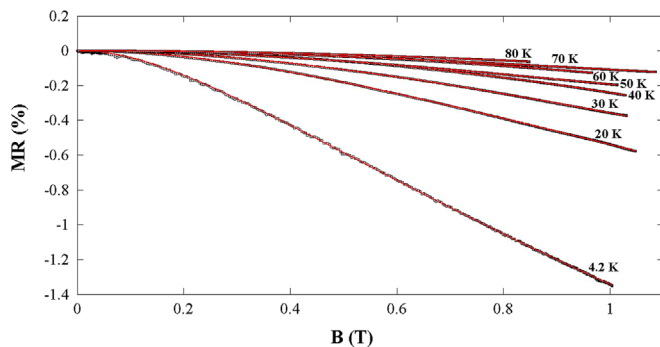
As can be seen from Fig. 4, the fit superimposed well on the experimental data. Moreover, the fit using Eq. (3) also superimposed well on the experimental data. The fitting parameters  $\alpha$  for Eq. (2) and Eq. (3) are given in Table 1.

Fig. 5 shows the phase-coherence length temperature dependence obtained from parameter  $B_\phi$ .

The phase-coherence length temperature dependencies obtained from the 2D and 3D weak theories are similar as shown in Fig. 5. However, there are differences in the absolute values of the



**Fig. 3.** The magnetoresistance of the In<sub>2</sub>O<sub>3</sub> thin film versus external perpendicular and parallel magnetic fields measured at 4.2 K (a) and 80 K (b).



**Fig. 4.** The magnetoresistance of the  $\text{In}_2\text{O}_3$  thin film versus the magnetic field. The open squares are experimental data and the red solid line is a fit using Eq. (2). (For interpretation of the references to color in this figure legend, the reader is referred to the web version of this article.)

**Table 1**  
Value of fitting parameters  $\alpha$  for Eqs. (2) and (3).

Temperature (K)	$\alpha$ for Eq. (2)	$\alpha$ for Eq. (3)
4.2	0.519	3.327E-08
20	0.605	2.981E-08
30	0.748	2.643E-08
40	17.32	4.888E-08
50	0.365	1.981E-08
60	13.48	5.094E-08
70	0.213	1.007E-08
80	0.7385	1.839E-08

phase-coherence length. Furthermore, these temperature dependencies were fitted by the function  $l_\phi = aT^p$ . For 2D and 3D,  $a$  was 52.04 and 69.11, and  $p$  was  $-0.3517$  and  $-0.3543$ , respectively.

These  $p$  values agree well with the theory of electron-electron interaction with small energy transfer in 1D systems (theoretical  $p = -1/3$ ) [28]. This means that the phase-coherence length temperature dependence is a sign of electron-electron scattering. This is an interesting observation, because a similar power law of  $l_\phi$  has been observed in recent experimental studies of 1D structured materials [32,50–55].

A surprising fact was that the phase-coherence length at increasing temperatures began to oscillate around 30 K for both curves (Fig. 5a and b). After analyzing experimental works on the study of phase-coherence length temperature dependence in structured materials [29,30,54,56–61], we have concluded that if

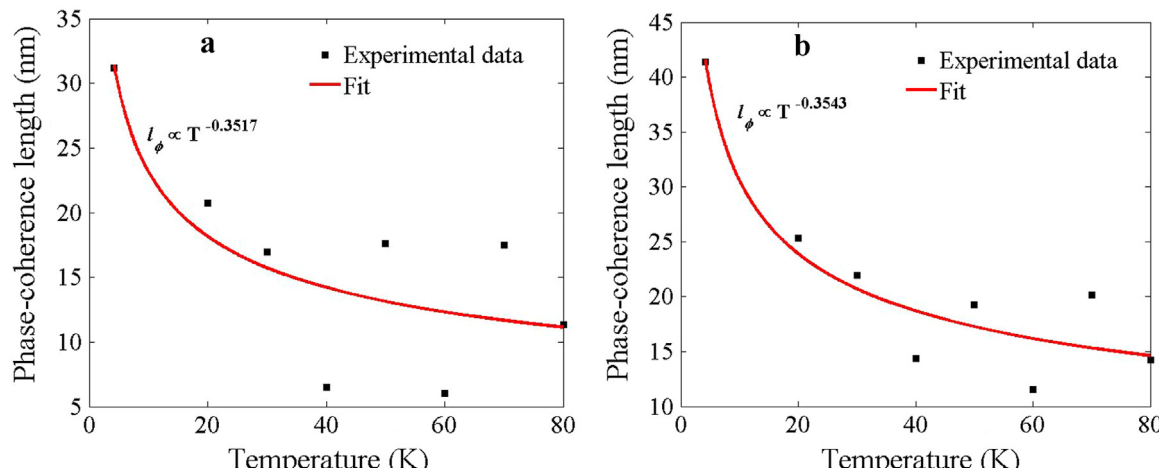


**Fig. 5.** The phase-coherence length temperature dependence for thin  $\text{In}_2\text{O}_3$  film obtained using (a) Eq. (2) and (b) Eq. (3), respectively. The black squares are experimental data and the red solid line is the fit. (For interpretation of the references to color in this figure legend, the reader is referred to the web version of this article.)

the phase coherence length begins is comparable to the geometrical dimensions of the structured material then such oscillations can be observed. However, in these experimental studies, this fact was given little attention because the oscillations were weak.

For phase-coherence length temperature dependence obtained from the 2D weak localization theory, the characteristic minimum values were 6.51 nm and 6.04 nm and the characteristic maximum values were 17.63 nm and 17.48 nm. For phase-coherence length temperature dependence obtained from the 3D weak localization theory, characteristic minimum values were 14.38 nm and 11.57 nm and the characteristic maximum values were 19.27 nm and 20.17 nm.

Based on the obtained the power law and the oscillation of the phase-coherence length, as well as the analysis of phase-coherence length minimum and maximum values, we have concluded that the thin indium oxide film is probably nanostructured and to has two structure characteristic parameters.

To test this statement, TEM investigations of thin  $\text{In}_2\text{O}_3$  film structural features has been done.

Fig. 6 presents TEM investigations of thin indium oxide film structural features in cross-section.

The film thickness of indium oxide was  $\sim 140$  nm as shown in Fig. 6a. First, from the standpoint of weak localization, the electron transport should be in the 3D WL regime. However, the structure of indium oxide has definite features as a «crystal phase – amorphous phase» as shown in Fig. 6b, i.e. the indium oxide film is nanostructured. In a number of articles [62–64], it was shown that the amorphous to crystalline transformation of the  $\text{In}_2\text{O}_3$  films occurs around 200 °C. Since we have limited the heating temperature to 200 °C, it is possible that there is not a complete transformation from the amorphous to the crystal phase in films. Thus, nanostructured  $\text{In}_2\text{O}_3$  films are obtained. Moreover, the crystalline phase characteristic size was  $\sim 20$ –30 nm and the amorphous phase characteristic size was  $\sim 6$ –10 nm. These characteristic values are already comparable to the phase-coherence length and thus phase-coherent electron transport with electron-electron interaction takes place, similar to 1D systems. Since phase-coherent electron transport takes place in the 1D regime, it becomes apparent why the observed the magnetoresistance is isotropic as shown in Fig. 3. Interference of the backscattered electronic wave functions occurs largely on the boundaries between crystalline and amorphous phases. Since phase-coherence length is comparable to the crystalline and phase characteristic sizes, the destruction of the interference (by using a magnetic field) is determined by the volume of the individual nano-crystal

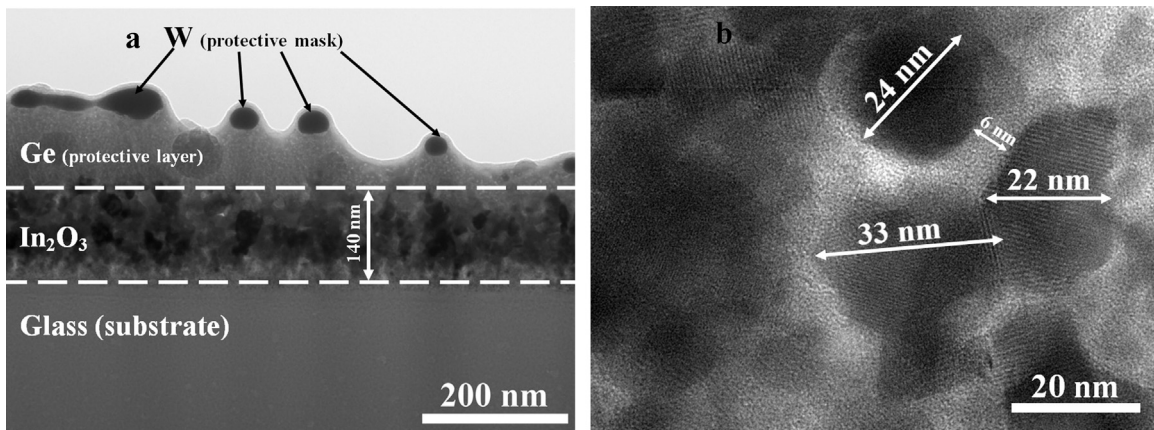


**Fig. 6.** Overview (a) and high-resolution (b) images of thin indium oxide film in cross-section.

or amorphous interlayer. The geometrical dimensions of the individual nano-crystal and amorphous interlayers are on the same order of magnitude. For this reason the destruction process of the interference using magnetic fields parallel and perpendicular to the film plane occur in a similar way. In addition, it can be assumed that the total destruction of the interference in the whole indium oxide film occurs as the sum of the destructions of interference in the individual nano-crystal and amorphous interlayers. Ultimately, we have a relatively large and isotropic magnetoresistance.

Of interest is the fact that the crystalline phase characteristic size is consistent with the maximum phase-coherence length and the amorphous phase characteristic size is consistent with the minimum phase-coherence length.

We hypothesized that if we consider the electron as a wave function, and take into account the effect of interference and the transmission coefficient in a structured system with two different materials of different thicknesses, then the same effect should be observed in visible optics. Indeed, in a number of experimental studies [65–67], similar effects of oscillation of transmittance have been observed. It should be noted that these oscillations, based on optical interference, are used to determine the film thickness [68].

Thus, we believe that the temperature measurements of the magnetoresistance as well as the theory of weak localization can be used to evaluate the structural features of nanocomposite or nanostructured thin films. In the future, we will try to use our finding to evaluate the structural features of thin nanocomposite Fe-In<sub>2</sub>O<sub>3</sub> [12], Fe-ZrO<sub>2</sub> [69] and Fe<sub>3</sub>O<sub>4</sub>-ZnO [70] films.

#### 4. Conclusions

In conclusion, we have synthesized thin In<sub>2</sub>O<sub>3</sub> films by the autowave oxidation reaction. A negative magnetoresistance was identified in the temperature range 4.2–80 K. At a temperature of 4.2 K and external magnetic field of 1 T, the thin In<sub>2</sub>O<sub>3</sub> film magnetoresistance was –1.35%. The negative magnetoresistance has been explained by the weak localization theory. WL theory was used to determine the phase-coherence length in the temperature range 4.2–80 K. It was found that the phase-coherence length at increasing temperatures began to oscillate around 30 K. It was suggested that the thin indium oxide film has two structure characteristic parameters. Transmission electron microscopy showed the structure of the thin In<sub>2</sub>O<sub>3</sub> film to have features of a «crystal phase – amorphous phase». It was found that the crystalline phase characteristic size is consistent with the maximum phase-coherence length and the amorphous phase characteristic size is consistent with the minimum phase-coherence length. It has been suggested that temperature measurements of the

magnetoresistance as well as the theory of weak localization can be used to evaluate the structural features of nanocomposite or nanostructured thin films.

#### Acknowledgments

This study was supported by the Russian Foundation for Basic Research (Grants # 16-32-00302 МОЛ\_а, # 15-02-00948-А, # 16-03-00069-А), by the Council for Grants of the President of the Russian Federation (SP-317.2015.1), and by the Program of Foundation for Promotion of Small Enterprises in Science and Technology (No. 6662ГУ2015, 9607ГУ/2015) (“UMNIK” Program). Electron microscopic studies were performed on the equipment of CCU KSC SB RAS.

#### References

- [1] J. Philip, A. Punnoose, B.I. Kim, K.M. Reddy, S. Layne, J.O. Holmes, B. Satpati, P. R. Leclair, T.S. Santos, J.S. Moodera, Carrier-controlled ferromagnetism in transparent oxide semiconductors, *Nat. Mater.* 5 (2006) 298–304.
- [2] S.X. Zhang, S.B. Ogale, W.Q. Yu, X.Y. Gao, T. Liu, S. Ghosh, G.P. Das, A.T.S. Wee, R. L. Greene, T. Venkatesan, Electronic manifestation of cation-vacancy-induced magnetic moments in a transparent oxide semiconductor: anatase Nb:TiO<sub>2</sub>, *Adv. Mater.* 21 (2009) 2282.
- [3] T. Fukumura, Z.W. Jin, A. Ohtomo, H. Koinuma, M. Kawasaki, An oxide-diluted magnetic semiconductor: Mn-doped ZnO, *Appl. Phys. Lett.* 75 (1999) 3366–3368.
- [4] F. Pan, C. Song, X.J. Liu, Y.C. Yang, F. Zeng, Ferromagnetism and possible application in spintronics of transition-metal-doped ZnO films, *Mater. Sci. Eng. Rep.* 62 (2008) 35.
- [5] Q. Li, L. Wei, Y. Xie, T. Zhou, G. Hu, S. Yan, J. Jiao, Y. Chen, G. Liu, L. Mei, Room temperature ferromagnetism in epitaxial In<sub>2</sub>O<sub>3</sub> films with embedded nano-sized Fe<sub>3</sub>O<sub>4</sub> columns, *Nanoscale* 5 (2013) 2713–2717.
- [6] T. Yu, P. Chen, Abnormal resistance and magnetoresistance temperature dependence in Fe-semiconductor granular films, *IEEE Trans. Magn.* 47 (2011) 3467–3469.
- [7] I.A. Tambasov, K.O. Gornakov, V.G. Myagkov, L.E. Bykova, V.S. Zhigalov, A. Matsynin, E.V. Yozhikova, Room temperature magneto-transport properties of nanocomposite Fe-In<sub>2</sub>O<sub>3</sub> thin films, *Physica B* 478 (2015) 135–137.
- [8] S. Yuasa, T. Nagahama, A. Fukushima, Y. Suzuki, K. Ando, Giant room-temperature magnetoresistance in single-crystal Fe/MgO/Fe magnetic tunnel junctions, *Nat. Mater.* 3 (2004) 868–871.
- [9] C. Chappert, A. Fert, F.R. Van Dau, The emergence of spin electronics in data storage, *Nat. Mater.* 6 (2007) 813–823.
- [10] J.J. Lin, Z.Q. Li, Electronic conduction properties of indium tin oxide: single-particle and many-body transport, *J. Phys. Condens. Matter* 26 (2014) 343201.
- [11] M.Z. Alam, I. De Leon, R.W. Boyd, Large optical nonlinearity of indium tin oxide in its epsilon-near-zero region, *Science* 352 (2016) 795–797.
- [12] V.G. Myagkov, I.A. Tambasov, O.A. Bayukov, V.S. Zhigalov, L.E. Bykova, Y. L. Mikhlin, M.N. Volochev, G.N. Bondarenko, Solid state synthesis and characterization of ferromagnetic nanocomposite Fe-In<sub>2</sub>O<sub>3</sub> thin films, *J. Alloy. Compd.* 612 (2014) 189–194.
- [13] J.J. Lin, J.P. Bird, Recent experimental studies of electron dephasing in metal and semiconductor mesoscopic structures, *J. Phys. Condens. Matter* 14 (2002) R501–R596.
- [14] Y.F. Tian, Y.F. Li, T. Wu, Tuning magnetoresistance and exchange coupling in ZnO by doping transition metals, *Appl. Phys. Lett.* 99 (2011) 222503.

